

# Joint Code-Frequency Index Modulation for IoT and Multi-User Communications

Minh Au<sup>1</sup>, *Member, IEEE*, Georges Kaddoum<sup>2</sup>, *Member, IEEE*, Md Sahabul Alam<sup>3</sup>, *Student Member, IEEE*, Ertugrul Basar<sup>4</sup>, *Senior Member, IEEE*, and Francois Gagnon<sup>5</sup>, *Senior Member, IEEE*

**Abstract**—In this paper we propose a family of index modulation systems which can operate with low-power consumption and low operational complexity for multi-user communication. This is particularly suitable for non-time sensitive Internet of Things (IoT) applications such as telemetry, smart metering, and soon. The proposed architecture reduces the peak-to-average-power ratio (PAPR) of orthogonal frequency-division multiplexing (OFDM)-based schemes without relegating the data rate. In the proposed scheme, we implement joint code-frequency-index modulation (CFIM) by considering code and frequency domains for index-modulation (IM). After introducing and analysing the structure of the CFIM, we derive closed-form expressions of the bit error rate (BER) performance over Rayleigh fading channels and we provide extensive simulation results to validate our outcomes. To better exhibit the particularities of the proposed scheme, the PAPR and complexity are thoroughly examined. The obtained results show that the PAPR is reduced compared to conventional OFDM-like IM-based schemes. Therefore, the proposed system is more likely to operate in the linear regime, which can in turn be implemented into low-cost devices with cost effective amplifiers. In addition, the concept is extended to synchronous multi-user communication networks, where full functionality is obtained by using orthogonal spreading codes. With the characteristics demonstrated in this work, the proposed system would constitute an exceptional nominee for IoT applications where low-complexity, low-power consumption and high data rate are paramount.

**Index Terms**—Code-frequency indexing, index-modulation, greedy detection, low-complexity, IoT, multi-user communication.

## I. INTRODUCTION

THE persistent demand for higher data rate communication systems associated with the increasing number of devices and gadgets for mobile Internet and Internet of Things (IoT) applications, is the challenge that needs to be addressed in the

next generation of wireless systems. Indeed, these networks are required to achieve high spectral efficiency (SE) while maintaining massive connectivity. For emerging devices such as drones and tiny sensors in intelligent vehicle technologies, ultra high reliability and extremely low-latency are absolute requirements.

Within the development of future wireless networks, the concept of IoT has emerged as the most promising technology that supports and enables many devices to gain Internet connectivity. This emerging technology has only become available via major advances in, and availability of tiny, and intelligent sensors that are cost-effective and easily deployable [1]. In addition, guaranteeing battery life saving through low energy consumption, is another noteworthy feature of these IoT devices. To fulfil these requirements, a large number of researchers have devoted themselves over the last decade [2]–[4].

Recently, the concept of index modulation (IM), which utilizes the indices of some transmission entities to carry extra information bits, has been proposed as a competitive approach for future wireless communications [5]–[7]. These IM-based systems aim to improve spectral efficiency (SE) and energy efficiency (EE) in emerging wireless communication devices [8]. In this direction, research in the last decade has seriously considered the use of certain parameters, such as space, polarity, code and frequency as modulation indices to enable the transmission of extra bits per symbol without demanding larger bandwidth or higher power.

In this vein, the spatial modulation (SM) technique, which is based on transitions between multiple antennas and using the index of the active antenna as a measure to carry extra information, is an area of growing interest where fruitful results have been provided [9]–[13]. However, this technique requires additional antennas to achieve more data rate. Although, SM scheme can be beneficial for IoT devices requiring high data rates, most low-cost and low-power IoT devices consider a simple transmission scheme using a single antenna (e.g. LoRa, NB-IoT, LTE-M).

Other examples of IM-based systems that use orthogonal frequency-division multiplexing (OFDM) include subcarrier-index modulation (SIM)-OFDM [14] and enhanced subcarrier-index modulation (ESIM)-OFDM [15]. However, these systems cannot compete with conventional OFDM systems.

A relatively stronger IM-based system that involves OFDM is the OFDM with index modulation (OFDM-IM), proposed in [16]. In this approach, the available subcarriers are grouped into many blocks where a subdivision of subcarriers contained in

Manuscript received December 30, 2018; revised April 19, 2019; accepted July 18, 2019. Date of publication August 9, 2019; date of current version October 14, 2019. The work of M. Au was supported by Dr. Richard J. Marceau Chair on Wireless IP Technology for Developing Countries and the Canada Research Chairs Tier 2. The work of E. Basar was supported by Turkish Academy of Sciences (TUBA) GEBIP Programme. The guest editor coordinating the review of this article and approving it for publication was Prof. Lina J. Karam. (Corresponding author: Minh Au.)

M. Au is with the Institute Research of Hydro-Québec, Varennes, QC J3X 1S1, Canada (e-mail: au.minh2@ireq.ca).

G. Kaddoum, M. S. Alam, and F. Gagnon are with the Department of Electrical Engineering, École de Technologie Supérieure, Montréal, QC H3C 1K3, Canada (e-mail: georges.kaddoum@etsmtl.ca; md-sahabul.alam.1@ens.etsmtl.ca; francois.gagnon@etsmtl.ca).

E. Basar is with the Communications Research and Innovation Laboratory, Department of Electrical and Electronics Engineering, Koç University, Sariyer 34450, Turkey (e-mail: ebasar@ku.edu.tr).

Digital Object Identifier 10.1109/JSTSP.2019.2933056

each block is *turned on* depending on indexing bits, while activated subcarriers transmit classical data symbols. This OFDM-based IM technique utilizes maximum likelihood (ML) detection at the receiver, which is indeed too complex for IoT and wireless sensor devices because low complexity operation and low power consumption are essential in these tiny gadgets. Fortunately, the log-likelihood ratio (LLR) detection method has been developed to achieve low complexity [16]–[18]. The obtained results show that the proposed LLR based detection scheme achieves near-ML performance while reducing complexity. However, in some IoT applications (e.g. smart home, smart metering, telemetry), the IoT devices require long battery life and low-cost deployment. Meanwhile, OFDM-like systems are known to have high peak-average-to-average power ratio (PAPR) which will require a more expensive high power amplifier to be considered in the design of those tiny gadgets.

In contrast to the aforementioned IM schemes, very low-complexity and low-power IM techniques have been recently proposed [19]–[25]. In the generalized code index modulation (GCIM) [19]–[21], extra information bits are carried by the selection of spreading codes. On the other hand, frequency index modulation (FIM) [22] is an OFDM scheme, in which extra bits are carried by the activation of one subcarrier, while the rest are nulled out. In [23], a low-complexity spread OFDM-IM-based system has been studied, allowing significant performance improvement by maximizing the transmission diversity through precoding matrices. Both data symbols of the active sub-carriers and their indices are spread and compressed to all available sub-carriers. In [24], a multicarrier index keying OFDM system using a low complexity greedy detection has been studied. This detection method is used with diversity reception employing several antennas at the receiver. In [25], a joint space-frequency IM-based system has been proposed, enabling the transmission of extra information bits with low-complexity detectors. Inspired by these low complexity detection methods, it is understood that choosing orthogonal spreading codes and frequencies and estimating those extra information bits by using square law energy detection (SLED) would significantly reduce the complexity at the receiver side.

Furthermore, from a multi-user communication perspective, given that 5G standards promise massive connectivity for billions of devices [26], [27], extensive research on IM schemes for multiple users has been recently carried out [28]–[32]. A multi-user IM scheme based on differential chaos shift keying (DCSK) has been proposed to enhance data security in [28], while a multi-user IM scheme based on a multi-carrier code division multiple access (MC-CDMA) framework has been proposed in [29]. The latter considers an orthogonal spreading code selector as an information-bearing unit. The resulting code sequence is spread over the subcarriers. The rest of the information is transmitted via an  $M$ -ary pulse amplitude modulation (PAM) or a quadrature amplitude modulation (QAM). The resulting vector is transmitted based on OFDM framework. While [32] employs a subset of transmitting antennas to carry extra information bits for single and multi-user communications, a non-orthogonal scheme with IM have been studied in [30], [31].

Although these multi-user IM schemes provide consistent results in terms of performance, they can exhibit high PAPR or require extra hardware (e.g. extra antenna in SM-based systems). Motivated by the design of low-power, low-complexity, and inexpensive IoT devices, one can exploit greedy detection techniques for low-complexity IM systems yielding a drastic reduction of the cost.

This paper exploits the benefits of having a joint code-frequency IM scheme that could meet the needs of 5G and beyond wireless systems to a great extent. The selection of the spreading codes and the frequency indices enable the use of very-low complexity greedy detection method such as SLED in multi-user scenario. This combination is particularly suitable for IoT applications where several sensors and devices must be connected.

The contributions of this paper are summarized as follows:

- A joint frequency and spreading code indexing mechanism is used as an information-bearing unit without adding extra hardware complexity to the system.
- An optimal receiver as well as a low-complexity detection method based on SLED are proposed.
- Closed-form mathematical expressions for the probability of bit error of CFIM are derived for greedy detection based on energy detection (ED) while an upper bound is derived for ML detection.
- The performance of CFIM is compared to other conventional low-complexity systems using greedy SLED and other IM-based approaches such as the direct spreading spectrum OFDM-IM (DSS-OFDM-IM) as well as parallel direct spreading CDMA (PDS-CDMA). The obtained results show that CFIM can outperform these schemes.

The remainder of this paper is organized as follows. Section II provides the system model of CFIM including the transmitter and receiver structures. Closed form expressions of the probability of bit error are analyzed in Section III. The PAPR and the complexity of the system are discussed in Section IV. CFIM is extended to synchronous multi-user communications in Section V. Section VI presents computer simulation results concerning the communication performance, the PAPR analysis and the complexity of the proposed scheme. Finally, conclusions follow in Section VII.

## II. SYSTEM MODEL

In this section, we present the CFIM transmitter and receiver architectures.

### A. The Transmitter

A typical architecture of the CFIM transmitter with  $KN$  subcarriers is depicted in Fig. 1. A sequence  $\mathbf{b}$  of  $p_T$  bits is equally separated into  $K$  blocks. Since each CFIM block has the same processing procedure, we consider the  $k$ th block for simplicity hereafter. In this block, the sequence  $\mathbf{b}_k = [\mathbf{b}_k^{p_1}, \mathbf{b}_k^{p_2}, \mathbf{b}_k^{p_3}]$  leaves the transmitter in chunks or sub-blocks of  $p$  bits where each sub-block consists of three sub-chunks such that  $p = p_1 + p_2 + p_3$ . Here,  $\log_2(M) = p_1$  denotes the number of modulated

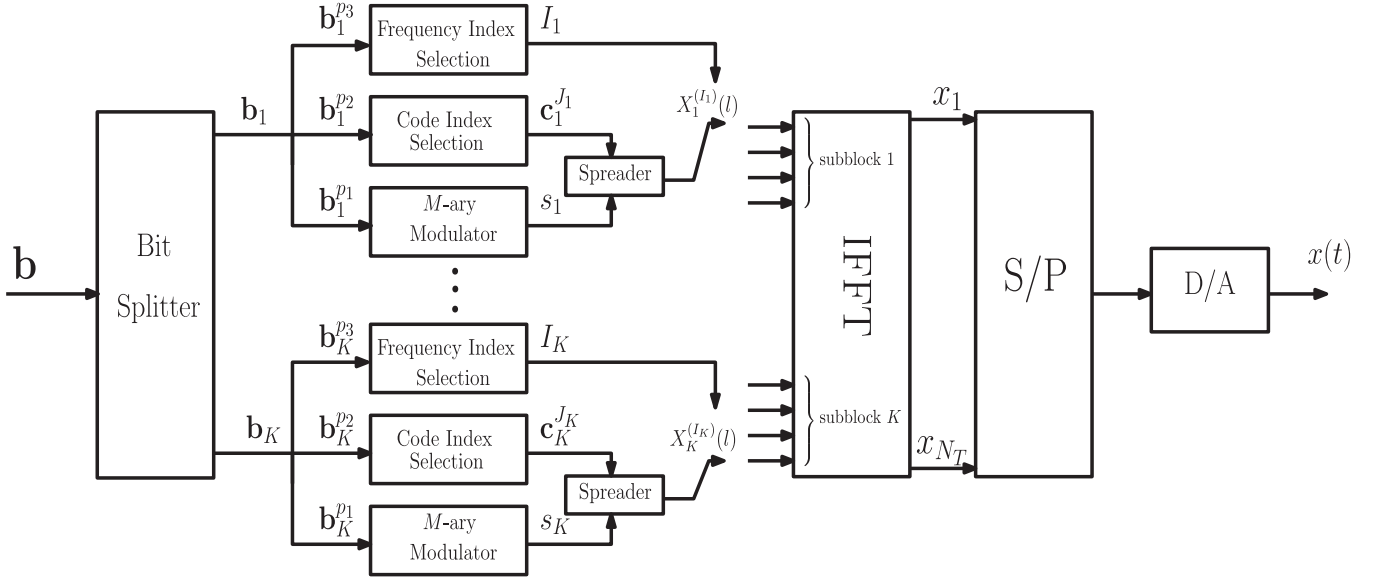


Fig. 1. CFIM architecture of the transmitter.

bits that are mapped into an  $M$ -ary signal constellation to produce a symbol  $s_k \in \mathcal{S}$ , where  $\mathcal{S}$  is a set of  $M$ -ary signals. Further,  $\log_2(N_c) = p_2$  is the number of mapped bits required to select the spreading code among  $N_c$  codes, and  $\log_2(N) = p_3$  is the number of mapped bits needed to activate one subcarrier. In this paper, we consider  $M$ -PSK modulation. It should be pointed out that when the CFIM transmitter uses  $K$  frequency resource blocks each containing  $N$  subcarriers, the transmission over OFDM is convenient because  $K$  frequencies are simultaneously activated. On the other hand, when one frequency resource block is used (i.e.  $K = 1$ ), then the IFFT complexity can be eliminated at the transmitter, since only a single carrier is activated.

The symbol  $s_k$  is spread over a single activated subcarrier by using a spreading code  $\mathbf{c}_k^{J_k}$  of length  $L$ . This code is indexed by  $J_k \in \mathcal{J}_k = \{1 \cdots N_c\}$  and indicates the selection of a code in a pool of  $N_c$  codes. The spreading code  $\mathbf{c}_k^{J_k} \in \mathbb{C}^L$  is selected from a predefined codebook in the block  $k$  denoted as  $\mathcal{C}_k = \{\mathbf{c}_k^1, \dots, \mathbf{c}_k^{N_c}\}$ . The signal is then transmitted via the subcarrier indexed by  $I_k \in \mathcal{I}_k = \{1 \cdots N\}$  out of  $N$  available subcarrier indices.

Since part of the transmitted bits are conveyed by the code and the frequency indices, and to have a fair comparison with other conventional systems, we define an equivalent system bit energy  $E_{bs}$  which represents the effective energy consumed per transmitted bit. This equivalent system bit energy is related to the physically modulated bit energy by the following relationship:

$$E_{bs} = \frac{p}{p_1} E_b. \quad (1)$$

It is worth mentioning that this definition will be used for the derivation of the closed-form expression of the CFIM BER performance.

Thus, the transmitted symbol has an energy per coded bit  $E_s = \mathbb{E}[s_k s_k^*] = p_1 E_{bs}$ . Due to their excellent correlation properties, orthogonal spreading codes such as Walsh-Hadamard

or Zadoff-Chu may be used. In this work, we employ Walsh-Hadamard codes, in which we have

$$\mathbf{c}_k^{J_k} \cdot (\mathbf{c}_k^{J'_k})^* = \sum_{l=0}^{L-1} c_k^{J_k}(l) (c_k^{J'_k}(l))^* = \begin{cases} L & \text{if } J_k = J'_k \\ 0 & \text{otherwise.} \end{cases} \quad (2)$$

where  $(\cdot)^*$  denotes the complex conjugate operation.

At the subcarrier  $i$ , the spread signal  $X_k^{(i)}(l)$  is given by:

$$X_k^{(i)}(l) = \begin{cases} s_k c_k^{J_k}(l) & \text{if } i = I_k \\ 0 & \text{otherwise.} \end{cases} \quad (3)$$

In particular, the subcarrier  $I_k$  contains the symbol  $s_k$  that has been spread by the selected code  $\mathbf{c}_k^{J_k}$ .

In addition, the orthogonality between the subcarriers holds in order to combat the intersymbol interference. This is given by  $\Delta f = 1/T_N \geq 1/T_c$  where  $T_N$  is the duration of a CFIM symbol, and  $T_c$  is the chip interval of the spreading code. Note that direct sequence spread spectrum is applied to each active subcarrier. Thus, the spreading operation is performed over time. This process is similar to PDS-CDMA systems.

Afterwards, the inverse Fast Fourier Transform (IFFT) is performed with an FFT length of  $N_T$ . Thus, the complete CFIM transmitting system that incorporates all blocks containing the symbols would be stated as:

$$x(t) = \frac{1}{\sqrt{T_N}} \sum_{k=1}^K \sum_{i=1}^N \sum_{l=0}^{L-1} X_k^{(i)}(l) p(t - lT_c) e^{j2\pi f_{i,k} t}, \quad (4)$$

where  $p(t)$  is a rectangular signaling pulse shifted in time given by

$$p(t) = \begin{cases} 1 & \text{if } 0 \leq t \leq T_c \\ 0 & \text{otherwise.} \end{cases} \quad (5)$$

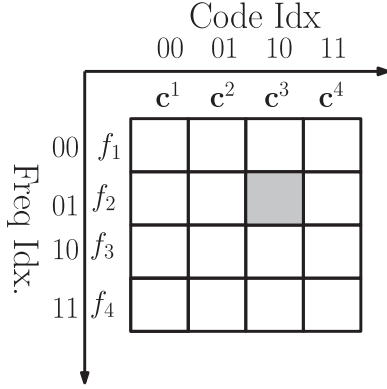


Fig. 2. An illustration of the CFIM system with 4 subcarriers and 4 codes where the transmitter has indexed the message 10 and 01. Then encodes the rest of the message via the spreading code  $\mathbf{c}_3$ , and transmits the encoded message via the subcarrier  $f_2$  only.

The subcarrier  $f_{i,k}$  is given by

$$f_{i,k} = \frac{N(k-1)}{T_N} + \frac{i}{T_N}. \quad (6)$$

Note that the active subcarrier is given by  $f_{I_k,k}$ , with  $i = I_k$ .

Moreover, the insertion and removal of the cyclic guard prefix is not expressed in our mathematical equations for the sake of simplicity. Fig. 2 illustrates the case where  $\mathbf{b}_k^{p_2} = [1, 0]$  and  $\mathbf{b}_k^{p_3} = [0, 1]$  which leads to the selection of the spreading code  $\mathbf{c}_3$ , and the selection of the second subcarrier, i.e.  $I_k = 2$  out of the 4 available subcarriers in the block.

### B. The Optimum Receiver

In this paper, frequency selective and time-invariant channels are considered, for which the chip interval  $T_c$  is larger than the maximum delay spread. Hence, the orthogonality of both the spreading codes and the subcarriers is ensured. Moreover, an additive white Gaussian noise (AWGN) is also considered. In this condition, the received spread signal denoted by  $Y_k^{(i)}(l)$  at the  $i$ th subcarrier for all  $l = 0, \dots, L-1$  in the  $k$ th block is given by

$$Y_k^{(i)}(l) = \begin{cases} s_k c_k^{J_k}(l) h_k^{(i)}(l) + Z_k^{(i)}(l) & \text{if } i = I_k \\ Z_k^{(i)'}(l) & \text{otherwise,} \end{cases} \quad (7)$$

where  $h_k^{(i)}(l) \sim \mathcal{CN}(0, 1)$  is the FFT output of the Rayleigh fading channel effect,  $Z_k^{(i)}(l)$  and  $Z_k^{(i)'}(l)$  are independent complex AWGN samples, with zero mean and variance  $N_0/2$ . In order to estimate the transmitted message in the  $k$ th block, we first consider a matrix of  $N \times L$  elements denoted by  $\mathbf{Y}_k$  such that

$$\mathbf{Y}_k = \begin{pmatrix} Y_k^{(1)}(0) & \dots & Y_k^{(1)}(L-1) \\ \vdots & & \vdots \\ Y_k^{(N)}(0) & \dots & Y_k^{(N)}(L-1) \end{pmatrix}. \quad (8)$$

The optimum receiver estimates the transmitted message by making a joint decision on the indices of the selected frequency

and spreading code, as well as the transmitted symbol. In fact, CFIM form a specific codeword by modulating a symbol and selecting the frequency and the spreading code. This codeword is a matrix that can be written as follows:

$$\mathbf{X}_k = \begin{pmatrix} X_k^{(1)}(0) & \dots & X_k^{(1)}(L-1) \\ \vdots & & \vdots \\ X_k^{(N)}(0) & \dots & X_k^{(N)}(L-1) \end{pmatrix} \quad (9)$$

where  $\forall i \in \{1, \dots, N\}$  and  $\forall l \in \{0, \dots, L-1\}$ ,  $X_k^{(i)}(l)$  satisfies (3). By using the maximum likelihood detection, the optimal decision is obtained by minimizing the following:

$$(\hat{s}_k, \hat{I}_k, \hat{J}_k) = \underset{i \in \mathcal{I}_k, j \in \mathcal{J}_k, s \in \mathcal{S}}{\operatorname{argmin}} \|\mathbf{Y}_k - \mathbf{X}_k \mathbf{H}_k\|_F^2. \quad (10)$$

where  $\|\cdot\|_F$  is the Frobenius norm,  $\mathbf{H}_k$  is an  $N \times L$  matrix representing the channel coefficients at the output of the FFT. It is worth mentioning that since the optimal receiver searches all possible combinations of  $\mathbf{X}_k$  for the one that minimizes (10), the computational complexity order is  $\sim \mathcal{O}(M N N_c)$ , which is of the same order of magnitude as for low-complexity ML detectors for SM [10]. For moderate values of  $M$ ,  $N$  and  $N_c$ , the optimal receiver can be too complex for IoT devices. Therefore, it is necessary to develop a CFIM receiver with low-complexity decoding.

### C. A Low-Complexity Receiver

A typical architecture of a low-complexity CFIM receiver with  $K$  activated subcarriers is depicted in Fig. 3.

In this case, the receiver uses a matrix  $\mathbf{c}_k = [\mathbf{c}_k^1, \dots, \mathbf{c}_k^{N_c}]^T$  of  $N_c \times L$  elements that contains the spreading codes in the codebook  $\mathcal{C}_k$  to despread the matrix  $\mathbf{Y}_k$ . Hence, the output of the despreader would simply be

$$\hat{\mathbf{X}}_k = \mathbf{Y}_k \mathbf{c}_k^H, \quad (11)$$

where  $(\cdot)^H$  denotes the Hermitian transpose operation. Then, a SLED is used to estimate both the active subcarrier and the selected code indices in the  $k$ th block. Since the spreading codes and the subcarriers are mutually orthogonal, the output variables of the matrix  $\hat{\mathbf{X}}_k$  are fed to the SLED forming an  $N \times N_c$  matrix  $\zeta_k$  of decision variables such that for  $i = 1, \dots, N$  and  $j = 1, \dots, N_c$  we have

$$\zeta_k^{(i,j)} = |\hat{X}_k^{(i,j)}|^2 = \begin{cases} |s_k h_k^{(i)} + \eta_k^{(i,j)}|^2 & \mathcal{H}_1 \\ |\eta_k^{(i,j)'}|^2 & \mathcal{H}_0, \end{cases} \quad (12)$$

where hypothesis 1,  $\mathcal{H}_1$  indicates the presence of the symbol  $s_k$ , and  $\mathcal{H}_0$  is the alternative hypothesis corresponding to the absence of a signal. The additive noise component  $\eta_k^{(i,j)}$  is given by

$$\eta_k^{(i,j)} = \sum_{l=0}^{L-1} Z_k^{(i)}(l) (c_k^j(l))^*, \quad (13)$$



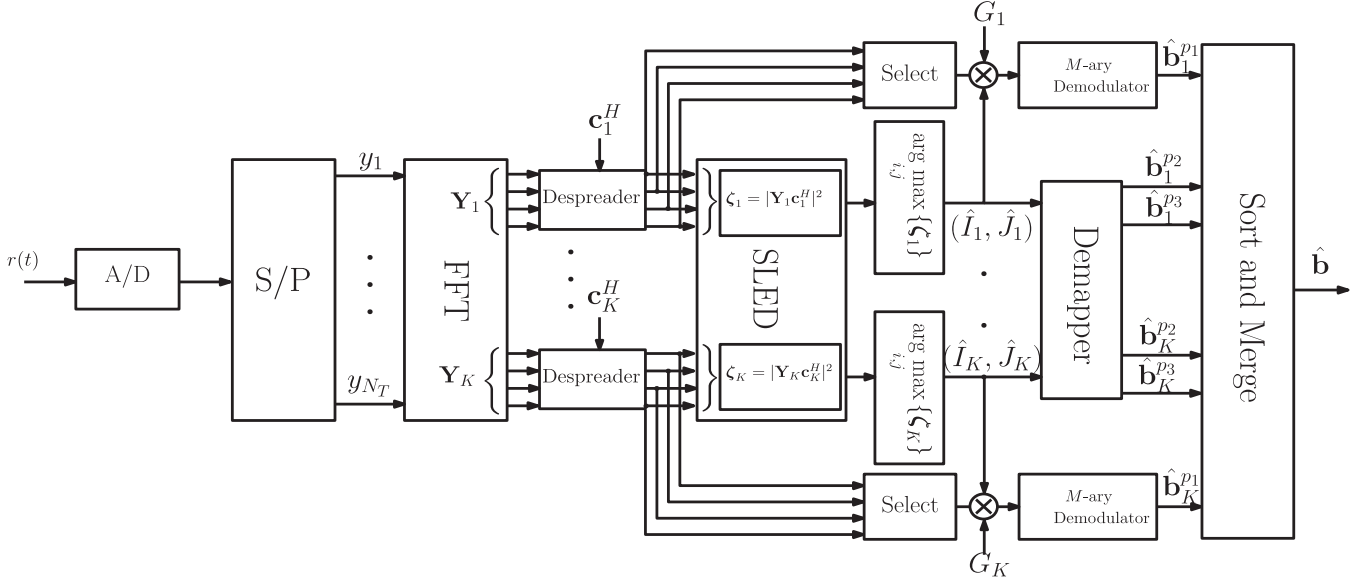


Fig. 3. CFIM architecture of the receiver.

and  $\eta_k^{(i,j)'}$  is obtained by substituting  $Z_k^{(i)}(l)$  by  $Z_k^{(i)'}(l)$  in (13). Since the AWGN components  $Z_k^{(i)}(l)$  and  $Z_k^{(i)'}(l)$  are mutually independent,  $\eta_k^{(i,j)}$  and  $\eta_k^{(i,j)'}$  are also independent.

In order to estimate the indices involved in the transmission, i.e.,  $(I_k, J_k)$ , the SLED chooses the arguments of the largest element of the matrix  $\zeta_k$  such that

$$(\hat{I}_k, \hat{J}_k) = \underset{i \in \mathcal{I}_k, j \in \mathcal{J}_k}{\operatorname{argmax}} \left\{ \zeta_k^{(i,j)} \right\}. \quad (14)$$

Therefore, the decision variable might land in  $\mathcal{H}_1$  if  $(\hat{I}_k, \hat{J}_k) = (I_k, J_k)$ . By estimating the active subcarrier and the selected code indices  $(\hat{I}_k, \hat{J}_k)$ , the receiver can extract the  $p_3 + p_2$  mapped bits. The receiver then demodulates the corresponding branch output using a conventional  $M$ -ary demodulator to extract the remaining  $p_1$  modulated bits. In this paper, we assume that the channel coefficients are perfectly estimated by the receiver. Thus, an equalization is performed at the receiver by dividing the received symbol  $\hat{X}_k^{(i,j)}$  by  $G_k = 1/h_k^{(i)}$ .

The receiver has two decision stages so that the complexity order is  $\mathcal{O}(M)$  for the modulation stage. Regarding the indices, the receiver needs to find the largest value of an array  $NN_c$ . By using the min heap algorithm, the complexity is  $\mathcal{O}(1)$ . Hence the overall complexity order of the system is  $\mathcal{O}(M)$ , which is valuable for low-complexity IoT devices.

### III. PERFORMANCE ANALYSIS

In this section, we investigate the performance of the CFIM system in terms of the probability of error obtained by concurrently mapping information bits into subcarrier and spreading code indices.

#### A. Probability of Bit Error Upper Bound for the ML Detector

An upper bound to the optimal CFIM receiver is derived in this paper. The conditional pairwise error probability is

given by:

$$P(\mathbf{X} \rightarrow \hat{\mathbf{X}}|\mathbf{H}) = Q\left(\sqrt{\frac{\|(\mathbf{X} - \hat{\mathbf{X}})\mathbf{H}\|_F^2}{2N_0}}\right) \quad (15)$$

where  $\hat{\mathbf{X}}$  is the estimated codeword. Following the method provided in [16], the unconditional pairwise error probability is given by approximating the  $Q$ -function as:

$$P(\mathbf{X} \rightarrow \hat{\mathbf{X}}) \approx \frac{1/12}{\det(\mathbf{I}_N + q_1 \mathbf{K}_N \mathbf{A})} + \frac{1/4}{\det(\mathbf{I}_N + q_2 \mathbf{K}_N \mathbf{A})} \quad (16)$$

where  $\mathbf{I}_N$  is the identity matrix,  $\mathbf{A} = (\mathbf{X} - \hat{\mathbf{X}})^H (\mathbf{X} - \hat{\mathbf{X}})$ ,  $\mathbf{K}_n = E[\mathbf{H}\mathbf{H}^H]$  is the correlation matrix of  $\mathbf{H}$ ,  $q_1 = 1/(4N_0)$  and  $q_2 = 1/(3N_0)$ . Therefore, the probability of bit error is upper bounded by:

$$P_u \approx \frac{1}{pn_{\mathbf{X}}} \sum_{\mathbf{X}} \sum_{\hat{\mathbf{X}}} P(\mathbf{X} \rightarrow \hat{\mathbf{X}}) e(\mathbf{X}, \hat{\mathbf{X}}) \quad (17)$$

where  $n_{\mathbf{X}}$  is the number of possible realizations of the codeword  $\mathbf{X}$  and  $e(\mathbf{X}, \hat{\mathbf{X}})$  is the number of the erroneous bit for the pair  $(\mathbf{X}, \hat{\mathbf{X}})$ .

#### B. Probability of Bit Error of the Low-Complexity CFIM System

In the CFIM scheme, the transmitted data in every block can be divided into three parts; two blocks to represent the mapped bits and a single block to identify the modulated bits. The former two blocks determine the combination of subcarrier and spreading code selected, while the latter block contains the remaining data.

In this structure, the probability of bit error of the CFIM system consists of the probability of bit error of the mapped bits  $P_{\text{map}}$  and the probability of bit error of the modulated bits  $P_{\text{mod}}$ . Subsequently, the probability of bit error of the system

could be described as

$$P_{\text{CFIM}} = \frac{p_1}{p} P_{\text{mod}} + \frac{p_2 + p_3}{p} P_{\text{map}}. \quad (18)$$

The probability of errors  $P_{\text{mod}}$  and  $P_{\text{map}}$  are respectively weighted by the number of modulated bits and the number of mapped bits and divided by the total number of bits involved in the transmission.

Moreover, these error probabilities are linked to the probability of erroneous detection of the code-frequency index pair,  $P_{\text{ed}}$ . Indeed,  $P_{\text{mod}}$  depends on the correct estimation of the selected indices and the probability of bit error of the  $M$ -ary modulation  $P_b$  when the indices are correctly estimated. Thereupon, errors happen in two different manners. The first case is when the selected indices are correctly estimated but an error takes place in the demodulation process. The second case is when an error befalls in the assessment of the indices chosen at the transmission, and the modulated bits are therefore estimated using inaccurate code-frequency indices. In this case, the receiver has no choice but to guess the modulated bits. In fact, the probability of bit error will be simply equal to  $1/2$ . Consequently, the bit error probability of the modulated bits would be expressed as:

$$P_{\text{mod}} = P_b(1 - P_{\text{ed}}) + \frac{1}{2} P_{\text{ed}}. \quad (19)$$

In the evaluation of  $P_{\text{map}}$ , the erroneous detection of the code-frequency index pair can cause a wrong estimation of the combination of mapped modulated bits. Each wrong combination can have a different number of incorrect bits compared to the correct combination, i.e., the actually transmitted one. Since, we have assumed that the frequency and the spreading codes are mutually orthogonal, the detection of the indices is simply equivalent to a noncoherent  $N \times N_c$ -ary orthogonal system upon which operates the SLED. Therefore, the probability of index in error  $P_{\text{ed}}$  is converted into the corresponding BER probability of mapped bits as

$$P_{\text{map}} = \frac{2^{(p_2+p_3-1)}}{2^{p_2+p_3}-1} P_{\text{ed}}. \quad (20)$$

*1) Probability of Erroneous Detection of the Code-Frequency Index:* Since a SLED is used for estimating the pair of indices, we shall determine the probability of erroneously detecting the code-frequency indices  $P_{\text{ed}}$  pair. To do so, we assume an equiprobable selection of the active subcarrier and the spreading code. Moreover, for the sake of clarity, we focus on a single block, i.e., the  $k$ th block such that  $\zeta_k^{(i,j)}$  of (12) simplifies to  $\zeta^{(i,j)} \forall i \in \mathcal{I}$  and  $\forall j \in \mathcal{J}$ . Moreover, since the frequency and the spreading codes are mutually orthogonal, we can write the matrix  $\zeta$  as a vector of  $NN_c$  elements, which is denoted as  $\text{vec}(\zeta) = [\zeta^{(1,1)}, \dots, \zeta^{(N,N_c)}] = [\zeta^{(1)}, \dots, \zeta^{(NN_c)}]$ .

Denoting the selected index at the transmitter as  $\nu$ , the probability of index error  $P_{\text{ed}}$  conditioned on the selected index  $\mu \in \{1, \dots, NN_c\}$  would be

$$P_{\text{ed}} = P \left\{ \zeta^{(\nu)} < \max_{\mu \neq \nu} \left( \zeta^{(\mu)} \right) \mid \nu \right\}, \quad (21)$$

for  $1 \leq \mu \leq NN_c$ .

Therefore, an error in the estimation of the selected index will occur if the decision variable  $\max(\zeta^{(\mu)})$  is larger than  $\zeta^{(\nu)}$ . In this condition, it is easy to show that  $P_{\text{ed}}$  is equivalent to the probability of detection of a noncoherent  $N \times N_c$ -ary orthogonal system over the Rayleigh channel. This is given by [33]:

$$P_{\text{ed}} = \sum_{\mu=0}^{NN_c-1} \frac{(-1)^\mu}{1 + \mu + \mu \bar{\gamma}_c} \binom{NN_c-1}{\mu}, \quad (22)$$

where  $\bar{\gamma}_c = \frac{\mathbb{E}[|h|^2]E_s}{N_0}$  is the average signal-to-noise ratio (SNR) per symbol, and  $h$  is the Rayleigh channel coefficient.

*2) Probability of Bit Error of Modulated Bits:* When the subcarrier and spreading code indices are correctly estimated, then we must consider the presence of the channel coefficient  $h$  when formulating the average bit error probability  $P_b$  of the modulated bit, which becomes conditional on the received power and may be drafted as

$$P_b = \int_0^{+\infty} P_{b|\gamma_b} P(\gamma_b) d\gamma_b, \quad (23)$$

where  $\gamma_b = \frac{|h|^2 E_{bs}}{N_0}$  is the instantaneous SNR per bit,  $P(\gamma_b)$  is the conditional probability distribution function (PDF) of  $\gamma_b$  given correct index estimation,  $P_{b|\gamma_b}$  is the conditional probability of bit error in AWGN channels [34]. Specifically, for an  $M$ -PSK modulation using Gray code, we may use the tight approximation, given in [35], to derive  $P_{b|\gamma_b}$ :

$$P_{b|\gamma_b} \approx \frac{1}{p_1} \sum_{u=1}^{M/2} w'_m P_m, \quad (24)$$

where  $w'_m = w_m + w_{M-m}$ ,  $w'_{M/2} = w_{M/2}$ ,  $w_m$  is the Hamming weight of the bits assigned to the symbol  $m$  as defined in [35], and  $P_m$  is given in (25).

$$P_m = \frac{1}{2\pi} \left\{ \int_0^{\pi(1-(2m-1)/M)} \exp \left( -p_1 \gamma_b \frac{\sin^2 [(2m-1)\pi/M]}{\sin^2 \theta} \right) d\theta - \int_0^{\pi(1-(2m+1)/M)} \exp \left( -p_1 \gamma_b \frac{\sin^2 [(2m+1)\pi/M]}{\sin^2 \theta} \right) d\theta \right\}. \quad (25)$$

In order to compute the probability of bit error  $P_b$ , the PDF of  $\gamma_b$  needs to be derived. It should be noted that the random variable  $\gamma_b$  is obtained knowing that the index estimation is correct. As a result, if the index estimation is always correct, i.e.,  $P_{\text{ed}} = 0$ , then  $\gamma_b$  is chi-square distributed with two degrees of freedom. This is due to the fact that  $h \sim \mathcal{CN}(0, 1)$ . In this case,  $P_b$  in (23) is equivalent to the probability of bit error of the conventional  $M$ -PSK over Rayleigh fading channels. However, in the low-SNR regime, SLED selects the index that has the greatest SNR. Consequently,  $\gamma_b$  is no longer chi-square distributed with two degrees of freedom. In this case, a closed form conditional probability distribution function  $P(\gamma_b)$  is not available. Nevertheless,  $P(\gamma_b)$  can be computed numerically.

By computing  $P_b$  using (24) and (25), the BER probability of the modulated bits  $P_{\text{mod}}$  can be obtained via (19). With  $P_{\text{map}}$  in (20), the comprehensive probability of bit error of the proposed  $P_{\text{CFIM}}$  scheme is presented in (18).

#### IV. PAPR, SPECTRAL EFFICIENCY AND COMPLEXITY ANALYSES

In this section, we consider the PAPR, the spectral efficiency, and the complexity analyses for the proposed CFIM system.

##### A. Analysis of the PAPR

A drawback of multicarrier systems is their PAPR. This causes distortions to the signal induced by the nonlinearity of high power amplifier (HPA) [36]–[38]; which impacts the performance, and also affects the spectral and energy efficiency of the system. Reducing the PAPR leads to significant power savings, which improves the energy efficiency. In fact, a high PAPR appears when a number of subcarriers in a given OFDM system are out of phase with each other. Thus, a high PAPR occurs when a large number of subcarriers is activated. It should be mentioned that such a scheme aims to save power without sacrificing the data rate. For a fair comparison, the same allocated power per subcarrier is considered for CFIM, PDS-CDMA and DSS-OFDM-IM.

By definition, the PAPR is defined as

$$\text{PAPR} = \frac{\max_{0 \leq t \leq T_N} |x(t)|^2}{1/T_N \int_0^{T_N} |x(t)|^2 dt}. \quad (26)$$

From (4), the maximum expected PAPR can be determined. In the PDS-CDMA, assuming that all symbols are equal, the peak value is given by

$$\max [x(t)x^*(t)] = \frac{E_s}{T_N} K^2 N^2 L^2, \quad (27)$$

while the mean square value of the signal is

$$\mathbb{E} [x(t)x^*(t)] = \frac{E_s}{T_N} K N L. \quad (28)$$

Therefore, the maximum expected PAPR of the PDS-CDMA is  $K N L$ . In CFIM, since a single subcarrier per block is activated, the maximum expected PAPR is  $K L$ . Therefore, the CFIM can reduce the PAPR by a factor of  $N$  compared to conventional PDS-CDMA. Since  $N = 2^{p_2}$ , the PAPR will significantly reduce as the number of bits  $p_2$  increases.

Since the CFIM scheme is an OFDM-like system associated with DSS, the signal  $x(t)$  is a point in an  $K L$  dimensional signal-space so that  $x(t)$  can be written as a vector  $\mathbf{x} = [x_1, \dots, x_{KL}]$ . For large  $K L$ , we assume that for  $i = 1, \dots, K L$ ,  $x_i \sim \mathcal{CN}(0, \sigma^2)$  where  $\sigma^2 = \mathbb{E} [x(t)x^*(t)]$  and  $x_i$  are independent and identically distributed. Under such a condition, the PAPR must be a random variable that follows the

TABLE I  
PAPR'S CDF OF OFDM-LIKE SYSTEMS

System	PAPR
CFIM	$(1 - e^{-\frac{r}{2\sigma^2}})^{K L}$
DSS-OFDM-IM	$(1 - e^{-\frac{r}{2\sigma^2}})^{K \kappa L}$
PDS-CDMA	$(1 - e^{-\frac{r}{2\sigma^2}})^{K N L}$

Rayleigh distribution. As a result, the joint cumulative distribution function (CDF) is given by:

$$\begin{aligned} F(r) &= \Pr \left( \max_{1 \leq i \leq K L} |x_i|^2 < r \right), \\ &= \Pr (|x_1|^2 < r) \Pr (|x_2|^2 < r) \cdots \Pr (|x_{K L}|^2 < r), \\ &= (1 - e^{-\frac{r}{2\sigma^2}})^{K L}. \end{aligned} \quad (29)$$

By taking the complementary cumulative distribution function (CCDF) of the PAPR, one can observe that the PAPR reduces since  $K$  out of  $K N$  subcarriers are activated for the transmission. In this case, the CFIM system is less likely to operate in a non-linear region. Moreover, this scheme does not require high power consumption and hence, it can be implemented into low-power and inexpensive devices, using low-cost power amplifiers. Considering  $K N$  subcarriers in the system, the CDF expressions of the PAPR for the CFIM, PDS-CDMA and DSS-OFDM-IM schemes are shown in Table I. It is worth mentioning that  $\kappa \leq N$  is the number of activated subcarriers in DSS-OFDM-IM systems.

##### B. Spectral Efficiency

We analyse the spectral efficiency of the proposed system by calculating its nominal spectral efficiency in bits/s/Hz. Since, CFIM systems exploit the OFDM framework combined with DSS, the length of the FFT, the cyclic prefix and the spreading factor should be taken into account. Furthermore, it has a total of  $K N$  subcarriers, but uses  $K$  subcarriers to transmit  $K p$  bits at every transmission instant. In fact one out of  $N$  subcarriers is activated in each block, so the spectral efficiency is obtained as

$$\begin{aligned} \xi_{\text{CFIM}} &= \frac{\log_2(M N_c N) K}{L(1 + \text{CP}) N_T}, \\ &= \frac{K p}{L(1 + \text{CP}) N_T}. \end{aligned} \quad (30)$$

where  $N_T$  is the FFT length and CP is the cyclic prefix length. Considering  $K N$  subcarriers in the system, the spectral efficiency values of the CFIM, PDS-CDMA and DSS-OFDM-IM schemes are given in Table II.

##### C. System Complexity

To evaluate the complexity of the proposed system, we provide the complexity of current state-of-the-art IM systems. First, we assume that all the presented IM schemes' parallel transmission consider DS-CDMA for multi-user communication. For instance, a parallel DS-CDMA in a conventional OFDM

framework becomes PDS-CDMA and the OFDM-IM with DSS is denoted as DSS-OFDM-IM.

The PDS-CDMA receiver makes a decision on a symbol for each activated subcarrier. In conventional OFDM, the complexity order is  $\mathcal{O}(M)$  per subcarrier. In DSS-OFDM-IM, an optimum receiver using ML detection and a log-likelihood ratio (LLR) detection method have been developed in [16]. Such a scheme considers multiple subcarriers indexes per block, the ML detector computes all possible combination of the subcarrier indexes and the modulated symbols resulting in a joint decision. In such a condition, the complexity order is  $\mathcal{O}(cM^\kappa)$  per block where  $c = 2^{\lfloor \log_2 \binom{N}{\kappa} \rfloor}$  and  $\kappa$  is the number of activated subcarriers out of  $N$ . For the large values of  $c$  and  $\kappa$ , the DSS-OFDM-IM ML detector can become impractical due to high complexity. Fortunately, [16], [17] have developed a LLR receiver that can operate in near-ML while reducing the complexity. Such scheme considers two-stage detection for which the selection of the indexes is obtained by finding the  $\kappa$  largest value in an array of  $N$ . By using the min heap algorithm, the complexity order is  $\sim \mathcal{O}(\kappa + (N - \kappa) \log \kappa)$ . Moreover, regarding the decision of the transmitted symbol, the complexity order is  $\sim \mathcal{O}(M)$  per subcarrier. It is worth mentioning that the calculation of the LLR detector for higher modulation orders  $M$ , requires all possible symbols [16]. A low-complexity LLR for OFDM-IM has been recently proposed for higher modulation orders  $M$  [18]. Applying it to the DSS-OFDM-IM, the complexity order of this low-complexity LLR detector becomes  $\mathcal{O}(\kappa M + \delta \varepsilon^\kappa)$  per block, where  $\delta$  is the parameter associated to the radius with the SNR, and  $\varepsilon$  is the parameter that determines the  $\varepsilon$ -th likely symbols are considered for the calculation of the LLR [18].

Considering  $KN$  subcarriers in the system, the complexity order of CFIM, PDS-CDMA and DSS-OFDM-IM schemes are depicted in Table III. It is worth mentioning that CFIM uses the OFDM framework by which only one subcarrier is activated and the rest are null. Hence, the system considers sparse matrices with which an even lower complexity can be obtained by computing sparse FFT. In this paper, we choose to implement the conventional FFT in order to compare the proposed CFIM with PDS-CDMA systems, which do not consider any sparsity vectors during the transmission.

## V. USING CFIM FOR SYNCHRONOUS MULTI-USER COMMUNICATIONS

In this section, we extend the proposed system to synchronous multi-user communications. First, we provide performance analyses of CFIM in multi-user scenario. Then, we provide a complete analysis in uplink and downlink transmission.

### A. Index Modulation for Multi-User Communications Using CFIM

Assuming that a codebook  $\mathcal{C}_k$  in the  $k$ th block can be split into a group of  $U$  codebooks of  $N_c$  orthogonal spreading codes each. In this condition, CFIM can be extend to multi-user communications where it operates in the same frequency band with no multi-user interference (MUI). Fig. 4 illustrates the case where

TABLE II  
SPECTRAL EFFICIENCY OF OFDM-LIKE SYSTEMS

System	Spectral efficiency
CFIM	$\frac{\log_2(MN_cN)K}{L(1+CP)N_T}$
DSS-OFDM-IM	$\frac{(\kappa \log_2(M) + \lfloor \log_2 \binom{N}{\kappa} \rfloor)K}{L(1+CP)N_T}$
PDS-CDMA	$\frac{\log_2(M)NK}{L(1+CP)N_T}$

TABLE III  
COMPLEXITY OF OFDM-LIKE SYSTEMS

System	Complexity
CFIM ML	$\mathcal{O}(KNMN_c)$
CFIM ED	$\mathcal{O}(KM)$
DSS-OFDM-IM ML	$\mathcal{O}(KcM^\kappa)$
DSS-OFDM-IM LLR $M = 2$	$\mathcal{O}(K(\kappa + (N - \kappa) \log \kappa + \kappa M))$
DSS-OFDM-IM LLR $M > 2$	$\mathcal{O}(K(\kappa M + \delta \varepsilon^\kappa))$
PDS-CDMA	$\mathcal{O}(KNM)$

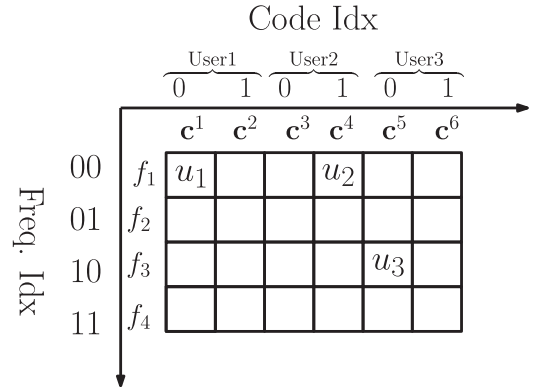


Fig. 4. The CFIM system with four subcarriers and two codes per user.

three users have two spreading codes each and four subcarriers are available for transmission. In the illustration, 00 has been indexed for User 1 and User 2, and thus  $f_1$  has been selected, while  $f_3$  has been selected for User 3. Regarding the spreading code selection,  $c_1$ ,  $c_4$  and  $c_5$  have been selected for User 1, 2 and 3, respectively.

Since the CFIM allows multiple users, we provide performance analyses for uplink and downlink transmission.

### B. Uplink Transmission

In uplink transmission, the users transmit  $U$  messages to the base station using CFIM transmitters. The base station has  $U$  CFIM receivers to decode those messages as depicted in Fig. 5. In this case, we assume that we allocate a single resource block of frequencies containing  $N$  subcarriers to a cluster of  $N_u$  users, and the base station aggregates all the data from all resource



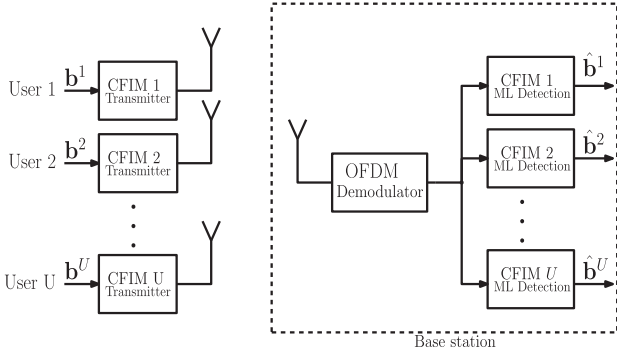


Fig. 5. Multiuser CFIM in uplink scenario.

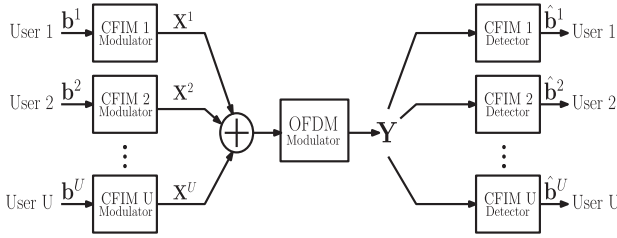


Fig. 6. Multi-user CFIM in downlink scenario.

blocks. Hence, for each user, a single-carrier CFIM transmitter is employed. Since we have assumed synchronous transmission, at the  $k$ th block and the  $i$ th subcarrier for all  $l = 0 \cdots L$ , the received spread signal at the base station is given by

$$Y_k^{(i)}(l) = \begin{cases} \sum_{u=1}^{N_{u,i}} h_{k,u} s_k^u c_k^{J_{k,u}}(l) + Z_k^{(i)}(l) & \text{if } i = I_{k,u} \\ Z_k^{(i)'}(l) & \text{otherwise,} \end{cases} \quad (31)$$

where  $h_{k,u}$  is the fading channel coefficient of the  $u^{\text{th}}$  user. It should be noted that the base station employs the optimal receiver by using a joint ML detection method as specified in Section II-B. Specifically, for  $U$  users, the base station decodes all the data from the  $U$  users by minimizing the following metric:

$$\begin{aligned} & (\hat{s}_k^1, \hat{I}_k^1, \hat{J}_k^1 \cdots \hat{s}_k^U, \hat{I}_k^U, \hat{J}_k^U) \\ &= \underset{\substack{i^u \in \mathcal{I}_k, j^u \in \mathcal{J}_k, s^u \in \mathcal{S} \\ \forall u=1 \cdots U}}{\operatorname{argmin}} \|\mathbf{Y}_k - \mathbf{X}_k \mathbf{H}_k^u\|_F^2. \end{aligned} \quad (32)$$

The complexity order of such a scheme is  $O((KNN_cM)^U)$ .

### C. Downlink Transmission

In downlink transmission, a base station prepares one message for each user using  $U$  CFIM modulators and transmits the overall signal, which is expected to be received by  $U$  independent receivers. In this case, it is convenient to transmit the data in the all resource blocks over OFDM. In synchronous transmission, MUI can be avoided by using orthogonal spreading codes. Fig. 6 illustrates the multi-user CFIM in the downlink scenario. It is worth mentioning that the base station can transmit up to  $U$  signals and the CFIM receivers operate using the low-complexity CFIM ED method.

Focusing on the  $k$ th block, the received spread signal at the  $i$ th subcarrier for all  $l = 0 \cdots L$  is given by

$$Y_k^{(i)}(l) = \begin{cases} h_k \sum_{u=1}^{N_{u,i}} s_k^u c_k^{J_{k,u}}(l) + Z_k^{(i)}(l) & \text{if } i = I_{k,u} \\ Z_k^{(i)'}(l) & \text{otherwise,} \end{cases} \quad (33)$$

where  $N_{u,i}$  is the total number of users whose combined signal is transmitted over the  $i$ th subcarrier. Moreover,  $s_k^u, c_k^{J_{k,u}}$  for  $l = 0 \cdots L - 1$  are respectively the modulated symbol and the spreading code selected by the  $u$ th user. Note that  $(I_{k,u}, J_{k,u})$  is the code-frequency index pair selected by the  $u$ th user.  $Z_k^{(i)}$  and  $Z_k^{(i)'}$  are the additive noise components at the  $i$ th subcarrier. In synchronous downlink scenarios, since orthogonal spreading codes are used, the detection of the transmitted signal for the  $u$ th receiver is similar to the single user CFIM receiver, as described in Section II-C. The complexity order of such a scheme is  $O(KM)$  per user.

## VI. NUMERICAL RESULTS

In this section, we study the derived analytical and simulation results for the proposed CFIM system and show that these results are in good agreement. Then we compare the performance of CFIM to other IM-based schemes like OFDM-IM systems in multi-user scenario. We also study the complexity and the PAPR of the proposed system. Finally, CFIM for multi-user communication in synchronous transmission is analyzed. In this paper, we have used a Walsh-Hadamard matrix with various sizes for spreading operations. Moreover, we have omitted the cyclic prefix for the sake of simplicity.

### A. Performance of CFIM

To yield a better understanding of the problem, in this subsection, we scrutinize for various scenarios of the parameters that affect the performance of the proposed CFIM. Since the modulation order  $M$ , subcarriers  $N$  and spreading codes  $N_c$  can be tuned, we shall consider the influence of each of these elements on the system performance.

We start by plotting the bit error rate (BER) performance of the CFIM scheme for various  $M$ ,  $N$  and  $N_c$  in Fig. 7. This theoretical performance is extracted from (18). We witness in this figure that analytical and simulation results for the CFIM system are in correspondence and great harmony, which validates our theoretical results. Moreover, increasing  $M$  reduces the Euclidean distance between the transmitted symbols and narrows down the decision zones at the receiver.

Furthermore, Fig. 7 also shows that our system is design-flexible and adaptable since  $M$ ,  $N$  and  $N_c$  can be tuned. We observe that the CFIM system with  $M = 2$ ,  $N = 4$ ,  $N_c = 2$  and one with  $M = 4$ ,  $N = 2$ ,  $N_c = 2$  both transmit four bits per transmission. However, the former one exhibits a better performance, because the modulated part transmits a single bit per symbol while the later transmits two bits per symbol.

The BER performance of CFIM with ML detection is depicted in Fig. 8. As observed in this figure, ML detection improves the performance of CFIM which is ideal for uplink scenarios. Such

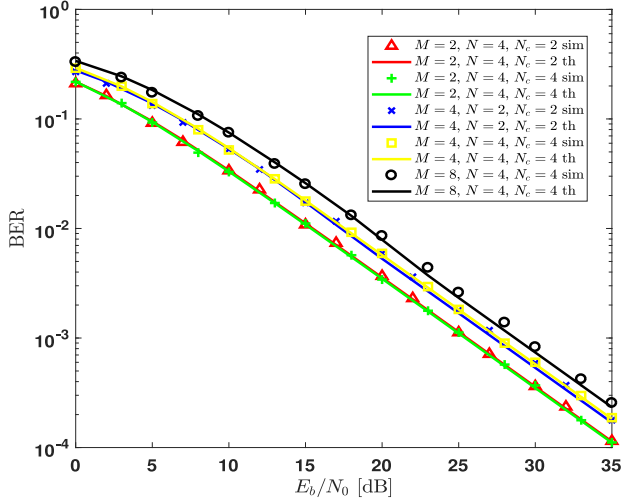


Fig. 7. Performance of CFIM ED over Rayleigh fading channels with a spreading factor of  $L = N_c$ .

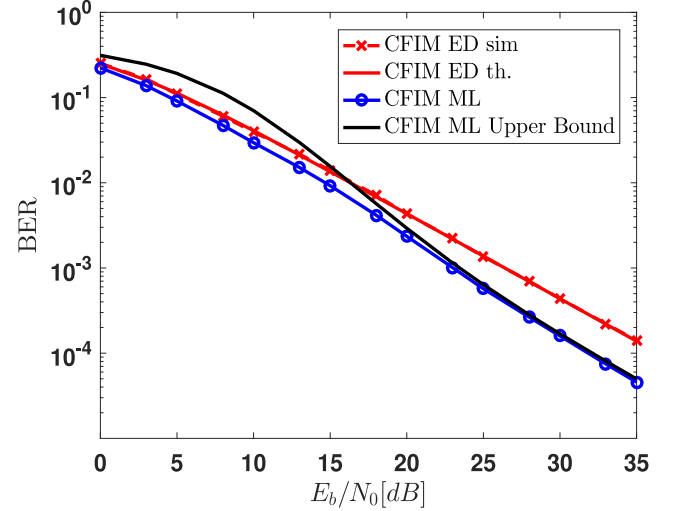


Fig. 9. Comparison of CFIM ED and CFIM ML detection with spreading factor of  $L = N_c$ .

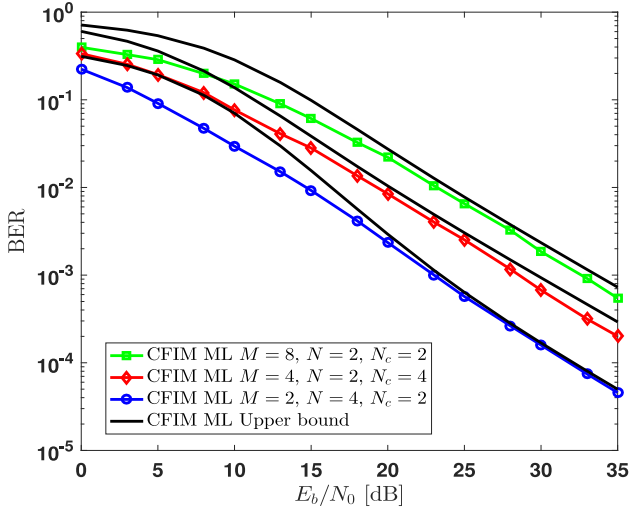


Fig. 8. Performance of CFIM ML detection with spreading factor of  $L = N_c$ .

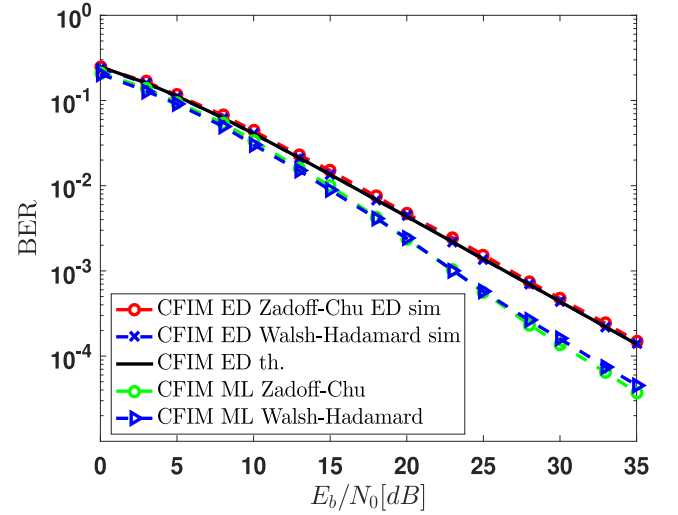


Fig. 10. Performance comparison between Zadoff-Chu and Walsh-Hadamard codes of CFIM with ED and ML detectors ( $M = 2, N = 4, N_c = 2, L = 4$ ).

a receiver can be implemented in a base station, which generally does not have any battery-life constraints. Also, the upper bound computed in (17) is tight in high  $E_b/N_0$  range. It can be used to approximate the CFIM performance in high SNR regime.

By comparing CFIM ED vs CFIM ML for  $M = 2, N = 4$ , and  $N_c = 2$  in Fig. 9, it is obvious that ML detection achieves better performance but will require more computational resources, which might not be suitable for low-cost IoT devices.

Since the Zadoff-Chu sequence is more commonly used in spread spectrum systems, the BER performance of the CFIM scheme is provided in Fig. 10 in comparison with Walsh-Hadamard codes. By ensuring the zero-autocorrelation of the Zadoff-Chu sequences with cyclically-shifted versions of itself, the CFIM receiver achieve similar performance to the CFIM with Walsh-Hadamard codes in both ED and ML detectors.

### B. Performance Comparison With IM Systems In Multi User Scenario

We compare the performance of the proposed scheme to that of relevant low-complexity and low-power multi-user systems such as FSK noncoherent using DS-CDMA, one carrier DS-CDMA and the DSS-OFDM-IM based schemes in which the base station transmit messages to low-complexity devices (downlink scenario). Moreover, we compare the performance of the CFIM in the uplink scenario in which the base station receives the signals from the users. In this case an ML detection is considered. For the comparison we choose to compare the performance of DSS-OFDM-IM and parallel-DS-CDMA.

Fig. 11 shows the performance of the proposed system in comparison to other IM-based schemes in downlink scenario. It is worth mentioning that all the systems in this case transmit

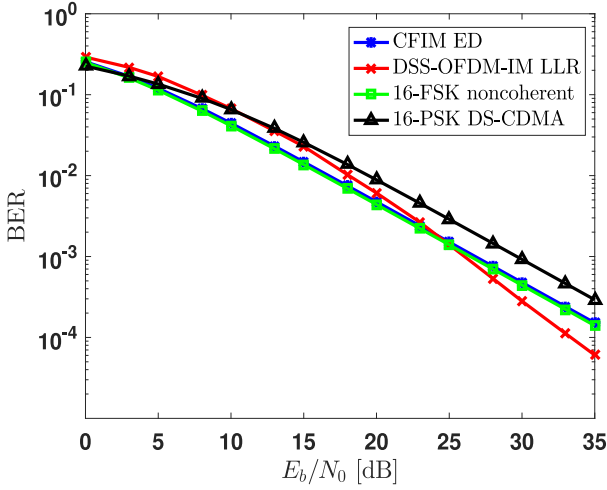


Fig. 11. Performance of CFIM in comparison to DSS-OFDM-IM, 16-FSK noncoherent and 16-PSK DS-CDMA for four bits per transmission in downlink 2 users case.

four bits per transmission using two sub-carriers out to four in the DSS-OFDM-IM and one subcarrier out to four in the CFIM and one single carrier for the rest of the systems. In order to transmit four bits, the CFIM uses the BPSK modulation, selects one subcarrier out to four and selects one spreading code for the indices while the DSS-OFDM-IM uses the BPSK modulation and activate two subcarriers out to four. In order to compare with conventional systems, we choose single-carrier 16-FSK and 16-PSK DS-CDMA and a spreading factor of  $L = 4$  for all the systems.

It is true that single-carrier systems can be more favourable to IoT scenarios because the IFFT complexity is eliminated at the transmitter and they have lower PAPR. However, the spectrum efficiency and/or the performance can be affected. Indeed, it can be seen that CFIM ED exhibits similar performance as 16-FSK noncoherent systems while requiring a smaller number of subcarriers compared to 16-FSK. Since CFIM has two degrees of freedom in the design (subcarrier and spreading codes), the system allows to use lower order of modulation, which reduces the complexity and improves the reliability compared to 16-PSK DS-CDMA. By comparing the DSS-OFDM-IM LLR, one can observe that CFIM ED is more effective in lower SNR range which is a typical range in low-power devices while DSS-OFDM-IM outperforms CFIM ED in higher SNR range.

Although DSS-OFDM-IM LLR outperforms other IM-based systems at  $E_b/N_0 = 25$  dB, CFIM exhibits a better BER performance in the low SNR regime. Therefore, CFIM can be beneficial in terms of performance in harsh environments. In IoT applications as well as in wireless sensor networks, communication can take place in industrial environments where transmission typically occurs in the low SNR regime. As a result, CFIM presents an ideal solution for this type of communication networks, where low transmission power consumption is an absolute requirement.

The CFIM scheme is compared to DSS-OFDM-IM and PDS-CDMA using ML detection. For example, if we take  $N = 4$  subcarriers, the FFT length  $N_T = 4$ , and the spreading factor

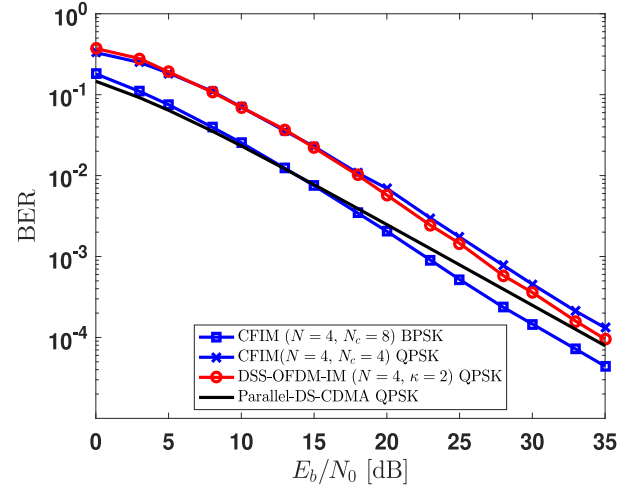


Fig. 12. Performance comparison of CFIM, DSS-OFDM-IM, and PDS-CDMA with FFT length  $N_T = 8$ ,  $N = 4$  subcarriers and spreading factor  $L = 8$  in uplink scenario.

$L = 8$  for all the systems. Under such conditions, by fixing the spectral efficiency for all the systems, the CFIM system can be implemented with either  $N_c = 8$  and  $M = 2$  or  $N_c = 4$  and  $M = 4$ . In the first case, the maximum of users is one while a maximum of two users can use the channel. For DSS-OFDM-IM, we use  $\kappa = 2$  which guarantees two extra bits that are used for the index and  $M = 4$ . For the PDS-CDMA all of the subcarriers are activated and  $M = 4$ . Hence, according to (30), the spectral efficiency is  $\xi = 0.1875$  Bit/s/Hz for all the systems. In Fig. 12, we show the performance of CFIM in comparison of DSS-OFDM-IM and PDS-CDMA using ML detection. One can observe that for QPSK modulation, CFIM and DSS-OFDM-IM show similar performance while the CFIM with BPSK can outperform PDS-CDMA for high  $E_b/N_0$  values.

CFIM is intended to reduce the PAPR while achieving low detection complexity in OFDM schemes by carrying extra information bits in both the frequency and code domains. In multi-user scenarios, frequency and spreading codes are radio resources, with which the CFIM system uses multiple codes and frequencies to carry extra information bits. By using orthogonal spreading codes, multiple users can exploit the same time-frequency resource for data transmission. However, CFIM can reduce the number of users supported because multiple codes can be allocated to one single user. Moreover, to support more users, one can consider additional spreading codes, but more resource time will be consumed, which is reasonable for non-time sensitive IoT applications such as smart metering and telemetry. The proposed IM-based system allows to carry extra information bits with more flexibility by indexing frequencies and/or spreading codes. Nevertheless, depending on the scenario, the allocated time-frequency resource must be taken into consideration in the design of the CFIM systems.

### C. PAPR and Complexity Analyses

Despite its simplicity, CFIM can achieve better spectral efficiency while maintaining higher reliability compared to other

TABLE IV

COMPLEXITY COMPARISON BETWEEN CFIM, DS-OFDM-IM AND PDS-CDMA SYSTEMS FOR MODULATION ORDER  $M = 2$ ,  $N = 4$  SUBCARRIERS, FFT LENGTH  $N_T = 4$ , AND SPREADING FACTOR  $L = 2$

	CFIM(4, 2)		DSS-OFDM-IM(4, 2)		PDS-CDMA
Spec Eff.	ML	ED	ML	LLR	ML
0.5 bps/Hz, BPSK	16	2	16	7.38	8

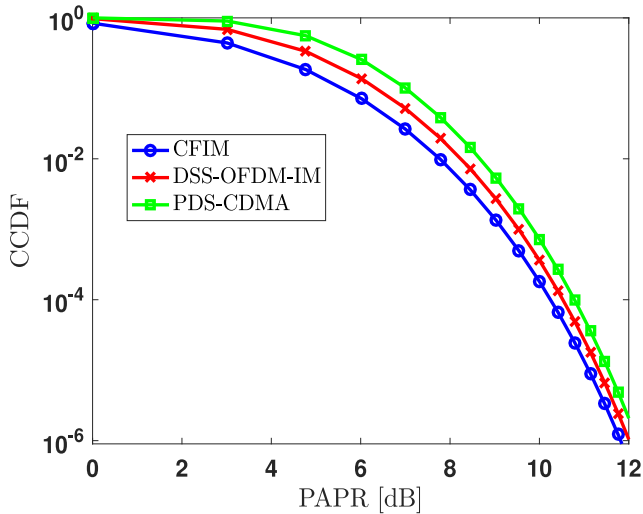


Fig. 13. CCDFs of the PAPR of the proposed CFIM in comparison with conventional DSS-OFDM-IM ( $N = 4$ ,  $\kappa = 2$ ) and PDS-CDMA for a spreading factor  $L = 4$ , number of blocks  $K = 1$ , number of subcarriers per block is  $N = 4$ , and FFT length  $N_T = 4$ .

IM-based systems. Moreover, CFIM as well as FIM schemes activate one subcarrier out of  $N$  subcarriers in a block, yielding communication systems with low-complexity and low-power consumption. These two criteria are paramount for IoT devices as well as for low-cost wireless sensors.

1) *System Complexity*: The computational complexity of these systems is considered for evaluation here. Since, CFIM can be applied to multi-user communications, we apply direct spread spectrum to other communication schemes in order to provide a fair comparison. In Table IV, the complexity of CFIM, DSS-OFDM-IM and parallel-DS-CDMA are provided. In this table, all the systems employ BPSK modulation, consider four subcarriers and the spreading factor is  $L = 2$ . Activating one subcarrier out of four and selecting one spreading code out of two, results in the lowest complexity when using the ED method, while the highest complexity is obtained using the ML detection. It can be seen that the complexity of DSS-OFDM-IM and CFIM in ML detection are quite similar.

2) *PAPR Analysis*: In order to complete the analysis, we have evaluated the PAPR of the proposed CFIM system in comparison with the aforementioned systems.

In Fig. 13, we have evaluated the CCDF of the PAPR for the proposed system in comparison with PDS-OFDM and DSS-OFDM-IM with  $N = 4$  and  $\kappa = 2$  systems. It can be seen that the CFIM has the lowest PAPR reduction. This is due to the fact that only one subcarrier per block is activated, which reduces the probability of having a high PAPR value.

## VII. CONCLUSIONS

In this paper, we proposed a low-complexity IM-based system that can significantly enhance the spectral and energy efficiencies while maintaining reliability. This scheme is based on a joint IM: code and frequency indexing. The proposed scheme suits IoT applications and can be extended to multi-user communications, where a remarkable performance has been shown in synchronous transmission.

The acquired closed-form expressions of the BER performance over fading channels is examined and validated by computer simulations. Moreover, analyses regarding complexity and PAPR analyses were performed, where our findings indicate a drop in the PAPR. This PAPR cutback shows the suitability of the proposed approach to sensor-based IoT applications, where the portrait of both power and complexity should be preserved at small values. The modulation architecture presented in this work satisfies the requirements of 5G-based wireless systems as it minimizes the PAPR and power consumption at the transmitter and demonstrates a satisfying overall performance in terms of reliability.

The proposed IM system is intended to be implemented in low-cost IoT devices that consider low-cost hardware circuits with low power linear amplifiers in general. Thus, we have considered a low complexity modulation scheme such as PSK modulation in the design. The analysis of high data rate CFIM-based system exploiting QAM modulation can be the subject of a future work.

Furthermore, some communication systems operate through asynchronous transmission. Under this condition, the performance severely degrades if orthogonal spreading codes such as Walsh-Hadamard or Zadoff-Chu sequences are used due to strong MUI. Therefore, using Gold codes will constitute an ideal alternative for such scenarios. Furthermore, most orthogonal multicarrier systems are sensitive to intercarrier interference caused by Doppler shift. Since CFIM systems are designed based on these two foundations, the overall performance may degrade. Therefore, performance analysis and mitigation techniques for these cases will be considered in future works.

## ACKNOWLEDGMENT

The authors would like to thank the anonymous reviewers for their valuable comments and suggestions to improve the quality of the paper. They are also grateful to the Hydro-Québec research institute (IREQ) team for their precious collaboration and their support.

## REFERENCES

- [1] P. Rawat, K. D. Singh, H. Chaouchi, and J.-M. Bonnin, "Wireless sensor networks: A survey on recent developments and potential synergies," *J. Supercomput.*, vol. 68, pp. 1–48, Apr. 2014.
- [2] S. Tozlu, M. Senel, W. Mao, and A. Keshavarzian, "Wi-Fi enabled sensors for internet of things: A practical approach," *IEEE Commun. Mag.*, vol. 50, no. 6, pp. 134–143, Jun. 2012.
- [3] Y. Chen, "Challenges and opportunities of internet of things," in *Proc. 17th Asia South Pacific Des. Autom. Conf.*, Feb. 2012, pp. 383–388.
- [4] C.-K. Toh, "Maximum battery life routing to support ubiquitous mobile computing in wireless ad hoc networks," *IEEE Commun. Mag.*, vol. 39, no. 6, pp. 138–147, Jun. 2001.



- [5] E. Basar, "Index modulation techniques for 5G wireless networks," *IEEE Commun. Mag.*, vol. 54, no. 7, pp. 168–175, Jul. 2016.
- [6] X. Cheng, M. Zhang, M. Wen, and L. Yang, "Index modulation for 5G: Striving to do more with less," *IEEE Wireless Commun.*, vol. 25, no. 2, pp. 126–132, Apr. 2018.
- [7] M. Wen, X. Vhang, and L. Yang, *Index Modulation for 5G Wireless Communications*. Berlin, Germany: Springer, 2017.
- [8] M. Wen, X. Cheng, M. Ma, B. Jiao, and H. V. Poor, "On the achievable rate of OFDM with index modulation," *IEEE Trans. Signal Process.*, vol. 64, no. 8, pp. 1919–1931, Apr. 2016.
- [9] R. Mesleh, H. Haas, C. Ahn, and S. Yun, "Spatial modulation: A new low complexity spectral efficiency enhancing technique," in *Proc. IEEE Conf. Commun. Netw.*, Oct. 2006, pp. 1–5.
- [10] J. Jeyadeepan, A. Ghrayeb, and L. Szczecinski, "Spatial modulation: Optimal detection and performance analysis," *IEEE Commun. Lett.*, vol. 12, no. 8, pp. 545–547, Aug. 2008.
- [11] R. Y. Mesleh, H. Haas, S. Sinanovic, C. Ahn, and S. Yun, "Spatial modulation," *IEEE Trans. Veh. Technol.*, vol. 57, no. 4, pp. 2228–2241, Jul. 2008.
- [12] M. D. Renzo, H. Haas, A. Ghrayeb, S. Sugiura, and L. Hanzo, "Spatial modulation for generalized MIMO: Challenges, opportunities, and implementation," *Proc. IEEE*, vol. 102, no. 1, pp. 56–103, Jan. 2014.
- [13] P. Yang, M. D. Renzo, Y. Xiao, S. Li, and L. Hanzo, "Design guidelines for spatial modulation," *IEEE Commun. Surv. Tut.*, vol. 17, no. 1, pp. 6–26, Jan. 2015.
- [14] R. Abualhiga and H. Haas, "Subcarrier-index modulation OFDM," in *Proc. IEEE 20th Int. Symp. Pers., Indoor Mobile Radio Commun.*, Sep. 2009, pp. 177–181.
- [15] D. Tsonev, S. Sinanovic, and H. Haas, "Enhanced subcarrier index modulation (SIM) OFDM," in *Proc. IEEE GLOBECOM Workshop*, Dec. 2011, pp. 728–732.
- [16] E. Basar, U. Aygolu, E. Panayirci, and H. V. Poor, "Orthogonal frequency division multiplexing with index modulation," *IEEE Trans. Signal Process.*, vol. 61, no. 22, pp. 5536–5549, Nov. 2013.
- [17] B. Zheng, F. Chen, M. Wen, F. Ji, H. Yu, and Y. Liu, "Low-complexity ML detector and performance analysis for OFDM with in-phase/quadrature index modulation," *IEEE Commun. Lett.*, vol. 19, no. 11, pp. 1893–1896, Nov. 2015.
- [18] H. Zeng, C. Fangjiong, W. Miaowen, J. Fei, and Y. Hua, "Low-complexity LLR calculation for OFDM with index modulation," *IEEE Wireless Commun. Lett.*, vol. 7, no. 4, pp. 618–621, Aug. 2018.
- [19] G. Kaddoum, Y. Nijssure, and H. Tran, "Generalized code index modulation technique for high-data-rate communication systems," *IEEE Trans. Veh. Technol.*, vol. 65, no. 9, pp. 7000–7009, Sep. 2016.
- [20] G. Kaddoum, M. Ahmed, and Y. Nijssure, "Code index modulation: A high data rate and energy efficient communication system," *IEEE Commun. Lett.*, vol. 19, no. 2, pp. 175–178, Feb. 2015.
- [21] G. Kaddoum and E. Soujeri, "On the comparison between code-index modulation and spatial modulation techniques," in *Proc. Int. Conf. Inf. Commun. Technol. Res.*, May 2015, pp. 24–27.
- [22] E. Soujeri, G. Kaddoum, M. Au, and M. Hercerg, "Frequency index modulation for low complexity low energy communication networks," *IEEE Access*, vol. 5, pp. 23 276–23 287, 2017.
- [23] T. V. Luong and Y. Ko, "Spread OFDM-IM with precoding matrix and low-complexity detection designs," *IEEE Trans. Veh. Technol.*, vol. 67, no. 12, pp. 11 619–11 626, Dec. 2018.
- [24] J. Crawford, E. Chatziantoniou, and Y. Ko, "On SEP analysis of OFDM index modulation with hybrid low complexity greedy detection and diversity reception," *IEEE Trans. Veh. Technol.*, vol. 66, no. 9, pp. 8103–8118, Sep. 2018.
- [25] S. Gao, M. Zhang, and X. Cheng, "Precoded index modulation for multi-input multi-output OFDM," *IEEE Trans. Wireless Commun.*, vol. 17, no. 1, pp. 17–28, Jan. 2018.
- [26] F. Boccardi, R. H. Jr., A. Lozano, T. Marzetta, and P. Popovski, "Five disruptive technology directions for 5G," *IEEE Commun. Mag.*, vol. 52, no. 2, pp. 74–80, Feb. 2014.
- [27] L. Dai, B. Wang, Y. Yuan, S. Han, C.-L. I, and Z. Wang, "Non-orthogonal multiple access for 5G: Solutions, challenges, opportunities, and future research trends," *IEEE Commun. Mag.*, vol. 53, no. 9, pp. 74–81, Sep. 2015.
- [28] M. Hercerg, G. Kaddoum, D. Vranjes, and E. Soujeri, "Permutation index DCSK modulation technique for secure multiuser high-data-rate communication systems," *IEEE Trans. Veh. Technol.*, vol. 67, no. 4, pp. 2997–3011, Apr. 2018.
- [29] Q. Li, M. Wen, E. Basar, and F. Chen, "Index modulated OFDM spread spectrum," *IEEE Trans. Wireless Commun.*, vol. 17, no. 4, pp. 2360–2374, Apr. 2018.
- [30] M. Yuzgecciglu and E. Jorswieck, "Transceiver design for GFDM with index modulation in multi-user networks," in *Proc. 22nd Int. ITG Workshop Smart Antennas*, Mar. 2018, pp. 1–4.
- [31] C. Zhong, Z. Hu, Z. Chen, D. W. K. Ng, and Z. Zhang, "Spatial modulation assisted multi-antenna non-orthogonal multiple access," *IEEE Trans. Wireless Commun.*, vol. 25, no. 2, pp. 60–67, Apr. 2018.
- [32] R. Rajashekar, K. V. S. Hari, and L. Hanzo, "Transmit antenna subset selection for single and multiuser spatial modulation systems operating in frequency selective channels," *IEEE Trans. Veh. Technol.*, vol. 67, no. 7, pp. 6156–6169, Jul. 2018.
- [33] J. G. Proakis, *Digital Communications*. New York, NY, USA: McGraw-Hill, 2001.
- [34] M. K. Simon and M. Alouini, *Digital Communication Over Fading Channels*. 2nd ed. Hoboken, NJ, USA: Wiley, 2005.
- [35] P. Lee, "Computation of the bit error rate of coherent M-ary PSK with gray code bit mapping," *IEEE Trans. Commun.*, vol. 34, no. 5, pp. 488–491, May 1986.
- [36] T. Jiang, C. Li, and C. Ni, "Effect of PAPR reduction on spectrum and energy efficiencies in OFDM systems with class-A HPA over AWGN channel," *IEEE Trans. Broadcast*, vol. 59, no. 3, pp. 513–519, Sep. 2013.
- [37] T. Jiang, M. Guizani, H. Chen, W. Xiang, and Y. Wu, "Derivation of PAPR distribution for OFDM wireless systems based on extreme value theory," *IEEE Trans. Wireless Commun.*, vol. 7, no. 4, pp. 1298–1305, Apr. 2008.
- [38] J. Armstrong, "Peak-to-average power reduction for OFDM by repeated clipping and frequency domain filtering," *Electron. Lett.*, vol. 38, pp. 246–247, Feb. 2002.



**Minh Au** received the bachelor's and M.S. degrees in computer science and telecommunication from the University of Poitiers, Poitiers, France, and the Ph.D. degree from the École de technologie supérieure, Montreal, QC, Canada. He has been actively involved in the Richard J. Marceau Industrial Research Chair for Wireless Internet in developing countries with Media 5 as a Postdoctoral Fellow. He is currently a Research Scientist with Hydro-Quebec Research Institute, Varennes, QC, Canada. His current research interests include channel modeling in harsh and hostile environments, partial discharge phenomenon, low-latency communication for machine-to-machine, information theory on coding theory and cybersecurity for smart grid.



**Georges Kaddoum** received the bachelor's degree in electrical engineering from the École Nationale Supérieure de Techniques Avancées (ENSTA Bretagne), Brest, France, and the M.S. degree in telecommunications and signal processing (circuits, systems, and signal processing) from the Université de Bretagne Occidentale and Telecom Bretagne (ENSTB), Brest, France, in 2005 and the Ph.D. degree (with honors) in signal processing and telecommunications from the National Institute of Applied Sciences (INSA), University of Toulouse, Toulouse, France,

in 2009. He is currently an Associate Professor and Tier 2 Canada Research Chair with the École de Technologie Supérieure (ÉTS), Université du Québec, Montréal, QC, Canada. Since 2010, he has been a Scientific Consultant in the field of space and wireless telecommunications for several US and Canadian companies. He has authored more than 200+ journal and conference papers and has two pending patents. His recent research activities cover mobile communication systems, modulations, security, and space communications and navigation. He was awarded the ÉTS Research Chair in physical-layer security for wireless networks in 2014, and the prestigious Tier 2 Canada Research Chair in wireless IoT networks in 2019. He was the recipient of the Best Papers Awards at the 2014 IEEE International Conference on Wireless and Mobile Computing, Networking, Communications, with three Co-Authors, and at the 2017 IEEE International Symposium on Personal Indoor and Mobile Radio Communications, with four Co-Authors. Moreover, he was the recipient of the IEEE Transactions on Communications Exemplary Reviewer Award for the year 2015 and 2017. In addition, he received the research excellence award of the Université du Québec in the year 2018. In the year 2019, he was the recipient of the research excellence award from the ÉTS in recognition of his outstanding research outcomes. He is currently serving as an Associate Editor for the IEEE TRANSACTIONS ON INFORMATION FORENSICS AND SECURITY and IEEE COMMUNICATIONS LETTERS.



**Md Sahabul Alam** received the bachelor's degree in electrical and electronic engineering from the Khulna University of Engineering and Technology, Khulna, Bangladesh, and the M.Sc. degree in telecommunications from the Institut National de la Recherche Scientifique, Université du Québec, Montréal, QC, Canada. He is currently working toward the Ph.D. degree in electrical engineering with the École de Technologie Supérieure, Université du Québec, Montréal, QC, Canada. His research interests include reliable wireless communications in non-Gaussian noise and interference typically modeled by impulsive noise, cooperative communications, and most specifically cooperative communications in impulsive noise environments. He has a special interest in smart grid with focus on designing robust communication systems, physical layer security, and NOMA for smart grid communications. During the Ph.D., he is awarded the prestigious FRQNT and NSERC postgraduate fellowships.



**Ertugrul Basar** (S'09–M'13–SM'16) received the B.S. degree (Hons.) from Istanbul University, Istanbul, Turkey, in 2007, and the M.S. and Ph.D. degrees from Istanbul Technical University, Istanbul, Turkey, in 2009 and 2013, respectively. He is currently an Associate Professor with the Department of Electrical and Electronics Engineering, Koç University, Istanbul, Turkey and the Director of Communications Research and Innovation Laboratory. His primary research interests include MIMO systems, index modulation, waveform design, visible light communications, and signal processing for communications. Recent recognition of his research includes the Science Academy (Turkey) Young Scientists (BAGEP) Award in 2018, Mustafa Parlar Foundation Research Encouragement Award in 2018, Turkish Academy of Sciences Outstanding Young Scientist (TUBA-GEBIP) Award in 2017, and the first-ever IEEE Turkey Research Encouragement Award in 2017.

Dr. Basar currently serves as an Editor for the IEEE TRANSACTIONS ON COMMUNICATIONS and *Physical Communication* (Elsevier), and as an Associate Editor for the IEEE COMMUNICATIONS LETTERS. He served as an Associate Editor for the IEEE ACCESS from 2016 to 2018.



**Francois Gagnon** received the B.Eng. and Ph.D. degrees from the École Polytechnique de Montréal, Montreal, QC, Canada. He was appointed to the position of Chief Executive Officer of the École de technologie Supérieure (ÉTS) in June 2019. He has been a Professor since 1991. Until very recently, he was the Director of the institut pour la résilience et l'apprentissage automatisé (Resilience and Computer-Assisted Learning Institute). He has held industrial research chairs since 2001. In addition to holding the Richard J. Marceau Industrial Research Chair for Wireless Internet in developing countries with Media5, he also holds the NSERC-Ultra Electronics Chair in Wireless Emergency and Tactical Communication. He also founded the Communications and Microelectronic Integration Laboratory and was its first Director. He has been very much involved in the creation of the new generation of high-capacity line-of-sight military radios offered by the Canadian Marconi Corporation, which is now Ultra Electronics TCS. Ultra-Electronics TCS and ÉTS have received the NSERC Synergy prize and an ADRIQ partnership prize for this collaboration. He was actively involved in the SmartLand project of UTPL, Ecuador, the STARACOM strategic research network, and recently with the Réseau Québec Maritime.